Journal of Materials Chemistry A

PAPER

View Article Online
View Journal | View Issue

Cite this: J. Mater. Chem. A, 2017, 5, 20860

Printing ultrathin graphene oxide nanofiltration membranes for water purification†

Mahdi Fathizadeh,[a] Huynh Ngoc Tien,[a] Konstantin Khivantsev,[a] Jung-Tsai Chen[a] and Miao Yu*[b]

Received 19th July 2017
Accepted 15th September 2017

DOI: 10.1039/c7ta06307e

rsc.li/materials-a

We demonstrated for the first time that inkjet printing can be a low-cost, easy, fast, and scalable method for depositing ultrathin (7.5–60 nm) uniform graphene oxide (GO) nanofiltration membranes on polymeric supports for highly effective water purification. A large area (15 × 15 cm^2) GO nanofiltration membrane was printed successfully on a modified polyacrylonitrile (M-PAN) support. Water permeance and rejection of small organic molecules (<1 nm, charged and uncharged) of printed GO membranes can be adjusted by controlling the GO "ink" concentration and/or printing time. Compared with commercial polymeric nanofiltration membranes, printed GO membranes, after optimization, showed approximately one order of magnitude higher water permeance and much higher rejection (>95%) of small organic molecules. Printed GO membranes also showed excellent performance in removing pharmaceutical contaminants, with ~95% rejection and <10% water permeance decline over extended-period permeation testing. We believe that inkjet printing could be an effective method for preparing ultrathin GO membranes for effective water nanofiltration purification.

Introduction

Graphene oxide (GO), a novel two-dimensional (2D) carbon-based material, has attracted a lot of attention recently with regard to the fabrication of water nanofiltration membranes; this is because of its excellent mechanical properties, atomically thin thickness, excellent dispersion in water, and ease of forming high-quality lamellar structures with sub-nanometer nanochannels.[1–5] Various solution-based deposition methods using water as an environmentally friendly solvent, including vacuum filtration,[6] pressurization,[7] drop-casting,[8] evaporation,[9] and spin coating,[10] have been used for depositing small-area GO membranes on porous substrates for water purification studies. Joshi *et al.*[11] used vacuum filtration to deposit approximately micrometer-thick GO membranes and found, by measuring liquid-phase diffusion rates of hydrated ions and dissolved organics, a sharp cut-off size of nanochannels at ~0.9 nm. Huang *et al.*[12] deposited 500 nm thick GO membranes by vacuum filtration and studied the effects of feed pressure, pH, and salt concentration on water filtration performance; they reported that low pH and high pressure (~1.3 MPa) resulted in the lowest water permeance but the highest Evans blue (EB) dye rejection, because of the narrowed interlayer spacing/nanochannels under these conditions. Sun *et al.*[8] used a drop-casting method to fabricate micrometer-thick (<10 μm) free-standing GO membranes that effectively separated Na^+ from Cu^{2+} by strong coordination interactions between heavy metal ions and functional groups of GO. These promising results on thick GO membranes demonstrated that nanochannels between GO flakes have potential for selective water purification. However, water permeance through these thick membranes was reported, and would be expected, to be low due to the high membrane thickness and, thus, high transport resistance.

Targeting higher water permeance, ultrathin GO membranes have been prepared and investigated for water purification. Han *et al.*[6] deposited ultrathin (22–53 nm), partially reduced GO membranes for nanofiltration by vacuum filtration of base-refluxing reduced GO dispersion. They obtained pure water permeance as high as 21.8 L m^{-2} h^{-1} bar^{-1} and >99% rejection for organic dyes, such as methyl blue (MB) and direct red 81 (DR). The ultrathin membranes also showed moderate rejection (20–60%) of salts with different cation to anion charge ratios. Hu *et al.*[6] prepared GO membranes of less than 50 layers by a novel layer-by-layer deposition process using 1,3,5-benzenetricarbonyl trichloride as a cross-linking agent. The resulting membrane showed high water permeance (8–27.6 L m^{-2} h^{-1} bar^{-1}), moderate rejection (46–66%) of MB, and high rejection (93–95%) of rhodamine-WT. These lab-scale, ultrathin GO membrane preparation methods, however, are either time-consuming or not scalable, or both, although the potential of such ultrathin, high-quality GO membranes for nanofiltration has been demonstrated. Recently, Akbari *et al.*[13] developed

[a]Department of Chemical Engineering, Catalysis for Renewable Fuels Center, University of South Carolina, Columbia, SC 29208, USA

[b]Department of Chemical and Biological Engineering, Rensselaer Polytechnic Institute, Troy, NY 12180, USA. E-mail: yum5@rpi.edu

† Electronic supplementary information (ESI) available. See DOI: 10.1039/c7ta06307e

a rapid (<5 s) and scalable casting method for depositing large-area (13 × 14 cm^2) GO membranes on a polymeric support; they obtained >90% rejection for organic molecules larger than ~1 nm (charged and uncharged) and 30–40% retention for monovalent and divalent ions. This casting method, however, produced relatively thick GO membranes (65–360 nm) using highly concentrated (40 mg mL^{-1}) and viscous GO paste that may not be stable over a long storage time; moreover, a significant amount of GO may be lost during the casting process. Additionally, it is challenging to cast a ~1 μm thick GO paste uniformly on large-area polymeric supports in a continuous process. Thus, an economic, relatively simple, fast, and scalable method for depositing ultrathin, high-quality GO nanofiltration membranes for highly permeable water purification application remains desirable.

Experimental section

Materials and chemicals

Single-layer graphene oxide (SLGO) powder (500–700 nm) was purchased from Cheap Tubes Inc. and characterized in our previous study.[14] All the chemicals, including pharmaceutical components (gemfibrozil, 17α-ethynylestradiol, diclofenac sodium salt, and iodixanol), salts (sodium chloride (NaCl), magnesium chloride ($MgCl_2$), magnesium sulfate ($MgSO_4$), and sodium sulfate (Na_2SO_4) with purity higher than 99%), concentrated sulfuric acid (H_2SO_4, 99.99%), potassium permanganate ($KMnO_4$, >99%), hydrochloric acid (HCl, 37%), and hydrogen peroxide (H_2O_2, 30% (w/w)) were purchased from Aldrich and used as received without further purification. Expandable graphite (Grade 1721-Asbury Carbon) was supplied by Asbury Carbon, and was used for synthesis of large GO flakes (>1 μm; see ESI† for experimental details). The PAN (M-PA400-GPET) ultrafiltration membrane, with a pore size of 20–50 nm, was purchased from Nanostone Water, Inc. P030 (Microdyn Nadir), TS40 (TriSep), and NF90 (Dow Filmtec) nanofiltration membranes were purchased from Sterlitech Corporation.

Modification of PAN. To prepare M-PAN, the PAN support was first immersed in 2 M NaOH solution at 50 °C for 30 min. Then, M-PAN was washed with DI water several times and stored in DI water for 24 h. M-PAN was dried at room temperature for 12 h before use for GO printing.

Printing GO coating

First, GO "ink" was prepared by dispersing 400 mg of SLGO in 100 mL DI water by ultrasonication for >2 h to ensure excellent dispersion of GO flakes in water. Then, the GO dispersion was centrifuged (5 min, 1000 rpm) to remove any large particles or aggregates. No obvious GO concentration change, as confirmed by UV-vis measurements, was observed before and after centrifugation, indicating a negligible amount of GO aggregates. Then, the supernatant was collected and diluted in DI water to prepare different concentrations of GO "ink". After making uniform GO "ink", a commercial Deskjet 1112 HP printer was used to print GO coatings on the surface of M-PAN support. For one-time printing, the printed GO membrane was dried for 12 h at room temperature and then 2 h at 80 °C; for multi-time printing, 4 h drying at room temperature was used between printings.

Characterization

Surface morphology and thickness of the printed GO coatings were examined by Field Emission Scanning Electron Microscope (FESEM) and Atomic Force Microscopy (AFM). Fourier transform infrared spectroscopy-attenuated total reflection (FTIR-ATR) spectroscopy was also used to investigate the functional groups of the PAN and M-PAN support surfaces. The water-contact angle was measured using a Ramé-Hart contact angle goniometer (Succasunna, NJ).

Permeation testing. A dead-end system was used for pressurized pure water permeation and salt/dye/pharmaceutical component rejection measurements, and a cross-flow system was used for the purification of water containing a pharmaceutical component (iodixanol) over an extended period. The concentrations of organic components in the feed and permeate were measured using a total organic carbon (TOC) analyzer (Tekmar Phoenix 8000-Persulfate), and salt concentration was measured using a conductivity meter (Pour Grainger International, Lake Forest, IL, USA).

Results

Printing GO on polymeric support

Here, for the first time we demonstrate an easy, fast, and scalable printing method using a conventional inkjet printer to deposit ultrathin, high-quality GO nanofiltration membranes on a polymeric support for effective water purification. We used a commercial HP ink cartridge (resolution: 1200 dots per inch, DPI) to hold an appropriate GO dispersion for printing (Fig. 1A); the inset field emission scanning electron microscopy (FESEM) image shows that the hole size of the cartridge nozzle was ~30 μm with a distance between holes in the same row of 90 μm and a distance between rows of 1000 μm (see Fig. S1† for more details). To develop an effective GO "ink" for printing, we identified two key properties of the GO dispersion: GO flake size and concentration. We found that dispersions with large GO flakes (>1 μm, prepared in our lab; see ESI† for more details) can readily block cartridge nozzle pores during printing, even at GO concentrations as low as 0.5 mg mL^{-1}, whereas dispersions with small GO flakes (~500 nm, purchased from Cheap Tubes Inc.) at the same concentration allowed smooth printing without blockages. With increasing GO concentrations, to higher than 4.0 mg mL^{-1}, ink blockage was observed even if small GO flakes were used. At GO concentrations below 0.5 mg mL^{-1}, "ink" leakage from cartridge nozzle pores was seen, apparently due to the lower viscosity of the GO dispersion (see Fig. S2† for more details). Thus, in this study we chose small, purchased GO flakes to prepare GO "ink" in the concentration range from 0.5 to 4 mg mL^{-1} for printing ultrathin GO membranes.

Modification of polymeric support layer

A hydrophilic surface of the polymeric supports was expected to be important to allow good wetting of the "ink" droplets and the

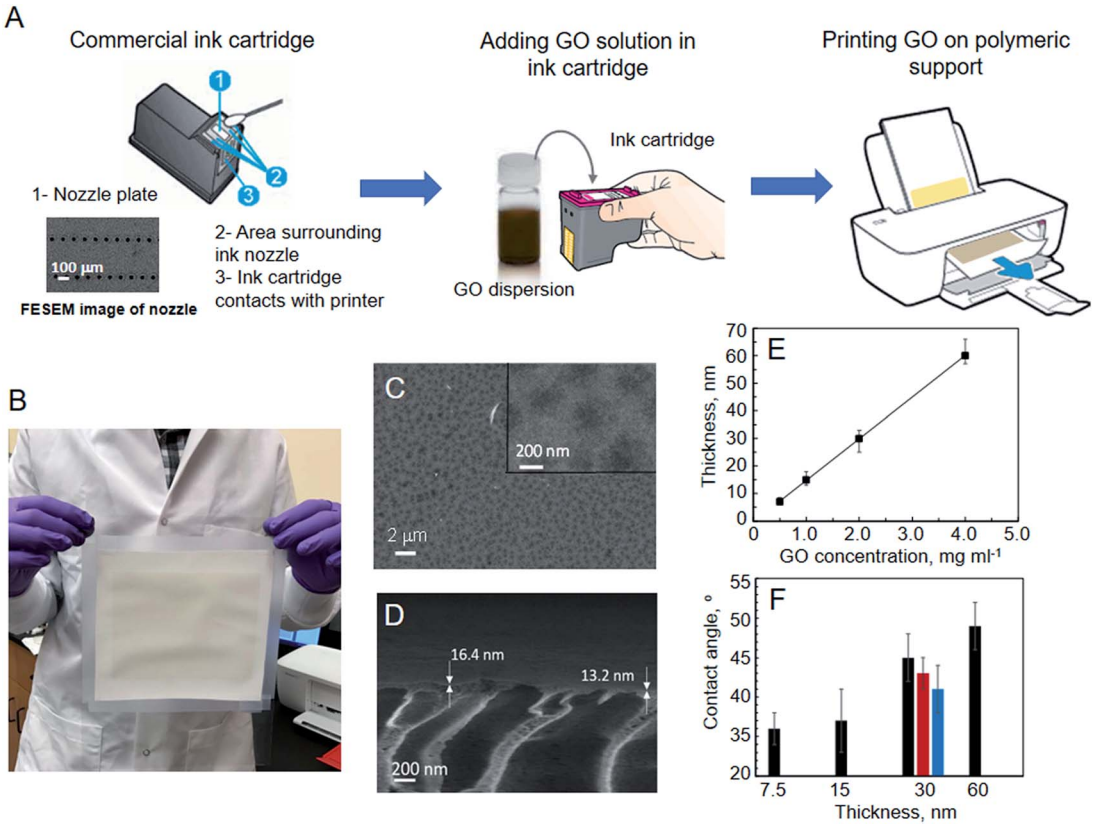

Fig. 1 Printed, ultrathin GO membranes. (A) Schematic showing the procedure for printing ultrathin GO membranes. (B) Digital picture of a printed GO membrane (15 × 15 cm^2) on modified PAN (M-PAN) support. (C) and (D) FESEM images of surface (C) and cross-sectional (D) views of a GO membrane printed using GO concentration of 1 mg mL^{-1} and with one-time printing; the inset in (C) shows the image at higher resolution. (E) Average printed GO coating thickness measured by FESEM as a function of GO concentration; one-time printing was applied. (F) Water contact angle as a function of average printed GO thickness; black column represents one-time printing, red column two-time printing, and blue column four-time printing.

subsequent merging of these droplets to form a continuous liquid film, to facilitate the deposition of uniform, continuous GO coatings (see proposed GO deposition mechanisms by printing in Fig. S3†). We selected polyacrylonitrile (PAN) ultrafiltration (UF) membranes with a skin-layer pore size of 20–50 nm as the base support for GO printing (Fig. S4A and C†). Poor and non-uniform GO coating on a PAN support after printing can be seen clearly, even with the naked eye (Fig. S5A†), and FESEM images (Fig. S5B and C†) showed areas with and without GO coating and obvious gaps between the areas. This was apparently due to the relatively hydrophobic PAN support surface (water-contact angle: 85°; Fig. S4A† inset) that resulted in poor wetting by the GO dispersion droplets and, thus, droplet separation. To improve the hydrophilicity, the PAN support was hydrolyzed with sodium hydroxide solution to form a more hydrophilic surface (Fig. S6†). After this surface modification, no obvious surface or pore-size change could be seen (Fig. S4B and D†), but the surface became more hydrophilic (water-contact angle: 35°; Fig. S4B† inset). Moreover, Fourier-transform infrared spectroscopy-attenuated total reflection (FTIR-ATR) spectra (Fig. S4E†) showed that the acrylonitrile (–CN) groups of the PAN support were converted to acid (–COOH) groups and amide (–CONH) groups during the hydrolysis process, which improved the surface hydrophilicity significantly.[15–17] GO coating on the modified PAN (M-PAN) by printing was uniform by visual examination (Fig. S5D†), and FESEM images (Fig. S5E and F†) showed a consistent uniform and thin GO coating, apparently due to the improved hydrophilicity of the M-PAN surface. Fig. 1B shows a digital picture of a representative, large area (15 × 15 cm^2), and uniform GO coating on the M-PAN support by the printing process (Video S1†), demonstrating great potential for scalable production of ultrathin GO membranes by this easy printing method. Fig. 1C shows the surface of an ultrathin, uniform GO coating on M-PAN support, printed using 1 mg mL^{-1} GO "ink". Compared with a blank M-PAN support (Fig. S4D†), M-PAN with a printed GO coating (Fig. 1C inset) does not have any exposed surface pores, indicating complete GO coverage on the support surface. A cross-sectional view of the printed GO coating (Fig. 1D) shows slight coating thickness variation, suggesting high uniformity of the printed GO coating.

Printed GO layer characterization

To investigate how well the printing method could control the average thickness, we took FESEM images of GO coatings

(Fig. S7A–F†) deposited using GO "ink" with different concentrations and with one-time printing. Fig. 1E shows the average GO coating thickness as a function of GO "ink" concentration after one-time printing; as expected, printed GO coating thickness increased linearly with the increase in GO concentration, indicating an easy way of controlling coating thickness. To further verify the average GO coating thickness and coating uniformity, we used atomic force microscopy (AFM) to measure the thickness of GO coatings printed using different GO concentrations and at different places (Fig. S7G and H; see ESI† for experimental details), and found results consistent with the FESEM images. We also calculated expected GO coating thickness (see ESI† for details), which was in good agreement with FESEM and AFM results. These experimental results clearly demonstrate that printing is an effective technology for producing ultrathin, uniform GO coatings with well-controlled thickness on appropriate porous supports.

Nanofiltration performance and water purification

Water wettability of the membrane surface is important for water permeation performance.[13,18] Fig. 1F shows the water-contact angle of GO coatings printed under different conditions. For one-time printing, water-contact angles were almost constant at 36–37° for 7.5 and 15 nm coatings, and then increased to 47° and 49° for 30 and 60 nm coatings, respectively. For a fixed GO coating thickness, multiple printing steps can also be used while reducing the GO concentration accordingly. At a fixed GO coating thickness of 30 nm, the water-contact angle decreased slightly, to 43° and 41° after two- and four-time printing, respectively. AFM measurements (Fig. S8†) of the GO coatings after one-time printing showed that the surface roughness decreased gradually, from 33.7 to 22.4 nm with an increase in GO coating thickness from 7.5 to 30 nm, and then increased to 31.4 nm for a 60 nm-thick GO coating. Because of the rough M-PAN support, a very thin GO coating (7.5 nm) conformally covers the support surface and replicates its relatively high roughness; with an increase in GO coating thickness to 30 nm, the relatively smooth GO coating dominates the surface roughness, but when further increasing the thickness, to 60 nm, the GO coating became rougher and surface roughness increased again. For a fixed GO coating thickness, multi-time printing seemed to have a negligible effect on surface roughness. FESEM images (Fig. S9†) showed that for one-time printing, a thin GO coating (15 nm) showed a conformal coating, replicating the support morphology, whereas thicker GO coatings (30 and 60 nm) had more characteristics of the GO coating itself; for multi-time printing of 30 nm coatings, slight surface morphology differences can be seen. It is known that surface roughness influences water wettability; according to the Wenzel equation, for a hydrophilic surface, water wettability improves with an increase in the nano-scaled surface roughness.[19] The trend in water-contact angles of printed GO coatings thus, generally, followed the Wenzel equation's prediction when GO membrane was thinner than 30 nm. For thicker GO coating (60 nm), it was less hydrophilic, although its roughness was larger than that of 15 and 30 nm GO coatings and comparable to that of 7.5 nm coating. FESEM images in Fig. S9† showed 60 nm coating had larger wrinkles (~micrometer-scale) than those of 15 and 30 nm coatings. Probably, surface morphology also has influence on the surface hydrophilicity, and relatively large wrinkles may lead to less hydrophilic surface. Similar phenomenon was found for 30 nm coatings deposited by different times of printing; with the decrease of printing time, less and larger wrinkles were found (Fig. S9†), which also led to less hydrophilic surface (Fig. 1F).

GO membranes printed under different conditions were evaluated for pure water permeation, rejection for dyes and pharmaceutical components, and brackish water desalination. Fig. 2A shows the pure water permeance (PWP) of GO membranes with different thicknesses and different printing times, measured using a dead-end system (Fig. S10†). For one-time printing, PWP increased slightly with the increase in coating thickness from 7.5 to 15 nm, although the coating thickness doubled, and then decreased markedly, 3.6 and 6.9 times, for 30 and 60 nm coatings, respectively. Recently, we found that the interlayer nanostructure of GO membranes with a lamellar structure plays an important role in water permeation; for GO membranes with the same thickness, self-assembly of GO flakes *via* a longer relaxation time consistently resulted in 2.5–4 times higher PWP and higher salt rejection, resulting from the more and narrower hydrophobic domains that allowed faster and more selective water permeation.[20] Compared with the 7.5 nm coating, the longer drying time of a 15 nm GO coating is expected; as a result, better self-assembled interlayer nanostructure, allowing faster water permeation, may form. The PWP of a 15 nm GO membrane, therefore, is actually higher than that of a 7.5 nm membrane, although it is twice as thick. For still thicker GO coatings (30 and 60 nm), although a better self-assembled interlayer nanostructure with a faster water permeation rate may result, the much thicker GO coating and, thus, higher transport resistance resulted in the greatly reduced PWP. For multi-time printed, 30 nm GO coatings, with the increase in printing time, PWP increases gradually, probably due to improved self-assembly during the multiple rounds of printing and drying processes. Thus, the PWP of printed GO membranes can be controlled by coating thickness and printing time, and optimized coating thickness and multi-time printing may greatly enhance PWP.

Both water permeance and rejection of small organic molecules are vital in evaluating nanofiltration membranes. We selected methyl orange (MO; molecular diameter: 0.79 nm; charge: −1) as a probe molecule to examine the quality of printed GO membranes by measuring its rejection (numbers above columns in Fig. 2A). Before each dye-rejection measurement, pure water permeation was conducted until a steady state permeance was obtained, and then dye filtration was performed; dye rejection after 2 h filtration was reported. Typically, water permeance decreased slightly, by ~15%, after the 2 h MO filtration testing. The thinnest 7.5 nm GO coating had the lowest rejection (79.6%), probably due to being too thin and, therefore, having occasional uncovered support pores (Fig. S11†). Increasing GO coating thickness increases MO rejection gradually, and the 60 nm GO coating showed the

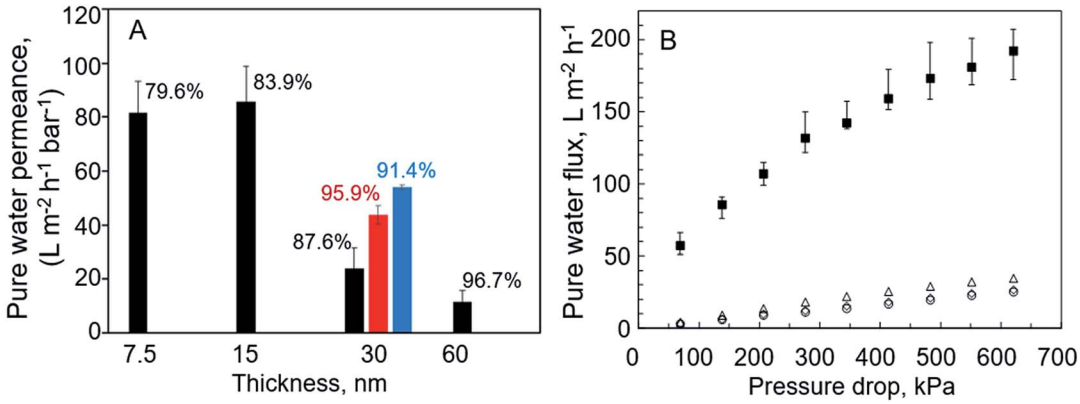

Fig. 2 Water permeation performance of printed GO membranes and comparison with commercial polymeric nanofiltration membranes. (A) Pure water permeance of printed GO membranes as a function of thickness and printing times; black column represents one-time printing, red column two-time printing and blue column four-time printing; numbers above each column are rejection of methyl orange (MO); pressure drop: 206.8 kPa (B) pure water flux of printed GO membrane (■: 30 nm, two-time printing) and commercial nanofiltration membranes (△: Microdyn Nadir; ◇: Trisep; ○: Dow Filmtec); MO rejections by membranes from Microdyn Nadir, Trisep and Dow Filmtec are 15.8%, 37.7% and 75.6%, respectively.

highest rejection, 96.7%. For 30 nm GO coatings, two-time printing resulted in comparable rejection to that of a 60 nm coating, but the PWP was 3.5 times higher. For 30 nm GO coatings, multi-time printing (2 and 4 times) generally led to improved rejection for MO, probably resulting from the narrower hydrophobic channels due to the better self-assembly during the drying (between printing) and rewetting (during printing) process. These MO rejection results indicated that the printed GO membranes had rejection performances in the nanofiltration range, and coating thickness and optimized printing time are important for controlling dye rejection.

To compare the nanofiltration performance of printed GO membranes with commercial nanofiltration membranes, we selected the 30 nm GO membrane with two-time printing because of its excellent MO rejection and moderate PWP. We also measured rejection of this GO membrane for charged and uncharged dyes with different molecular diameters to evaluate further its nanofiltration performance (Table 1); high rejection was obtained, suggesting excellent nanofiltration performance of the printed GO membrane. Three commercial nanofiltration membranes, from Microdyn Nadir, Trisep, and Dow Filmtec, were selected for water flux comparisons. Fig. 2B shows water flux *versus* pressure drop for the two-time printed, 30 nm GO membrane and the commercial nanofiltration membranes. The water flux of the printed GO membrane was about 10 times higher than that of the commercial nanofiltration membranes, whereas the commercial membranes had much lower MO rejection (Table S1† and caption in Fig. 2). These results indicated that the printed GO membranes have great potential for high permeance and high-rejection nanofiltration applications. The PWP and MO rejection of the printed GO membranes were comparable to, or higher than, those of reported GO membranes in the literature,[6,12,13,21–25] which were prepared by processes that are difficult to scale up (Table S2†). The printed GO membrane also showed similar salt rejection to reported GO membranes (Fig. S12† and discussion).

Pharmaceutical organic rejection. Another potential use of nanofiltration membranes is to remove contaminants of emerging concern (CECs) from water, including pharmaceuticals and personal care products, antibiotics, and endocrine-disrupting compounds, and their human-produced metabolites.[26,27] We evaluated the rejection of four different pharmaceutical contaminants by a two-time printed, 30 nm GO membrane after 2 h permeation in a dead-end system (Table S3†). The GO membrane showed excellent rejection, of 76.4, 80.1, 83.0, and 95.2% for gemfibrozil, 17α-ethynylestradiol, diclofenac sodium salt, and iodixanol, respectively. As a reference, most commercial polymeric nanofiltration membranes have rejections of <50% for these organic compounds.[28] Fig. 3 shows the nanofiltration performance of the printed GO membrane for removing iodixanol by a cross-flow system (Fig. S10†) over an extended operating period. In 120 h running, water permeance decreased by <10% with a slight decrease in rejection from >99% to 94% at 20 h, and was constant

Table 1 Dye rejection of two-time printed, 30 nm GO membrane

Dye molecule	Molecular diameter,[9] nm	Molecular weight, g mol^{-1}	Charge	Rejection, %
Methyl orange	0.79	327.3	−1	95.9
Riboflavin	0.83	376.3	0	97.6
Basic blue	0.86	359.89	1	96.3
Acid blue 45	0.84	474.33	−2	99.9
Acid blue 80	1.02	678.68	−2	>99.9%

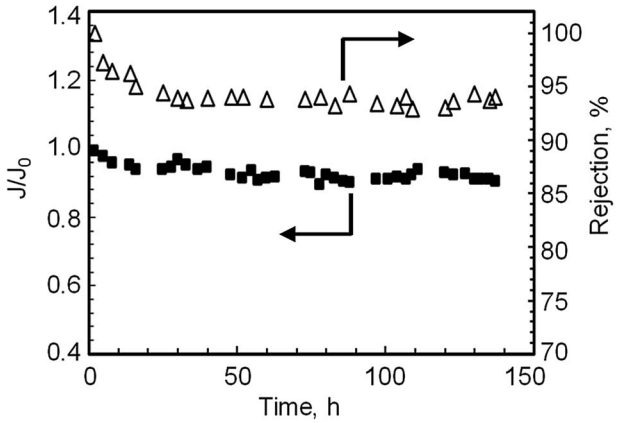

Fig. 3 Extended period nanofiltration performance testing for water containing a pharmaceutical contaminant (iodixanol; 10 ppm) by two-time printed, 30 nm GO membrane (J_0 = DI water permeability, J = iodixanol/water permeability).

thereafter. We also measured the feed concentration of iodixanol after collecting 100 mL permeate from 300 mL feed, and found that the ratio of final and initial concentrations was 1.29, suggesting that exclusion, not membrane adsorption, is the dominant mechanism for the high rejection. These results suggest that printed GO membranes have excellent stability and negligible fouling during nanofiltration testing.

Conclusions

In conclusion, we demonstrated for the first time that printing using a conventional inkjet printer is a low-cost, easy, fast, and scalable method for depositing ultrathin GO membranes for high water permeance and high-rejection nanofiltration. Water permeance and rejection for small organic molecules of the printed GO membranes can be tuned by adjusting the GO coating thickness and printing times. Compared with commercial nanofiltration membranes, the printed GO membranes showed approximately one order of magnitude higher water permeance and higher rejection of small organic molecules. The printed GO membranes also showed excellent nanofiltration performance for removing pharmaceutical contaminants in water and excellent long-term stability. We believe that inkjet printing could be a highly effective method for preparing ultrathin GO nanofiltration membranes for water purification.

Conflicts of interest

There are no conflicts to declare.

Acknowledgements

We gratefully acknowledge the support by National Science Foundation (NSF) Career Award under Grant No. CBET-1451887.

References

1 W. S. Hummers and R. E. Offeman, *J. Am. Chem. Soc.*, 1958, **80**, 1339.
2 J. R. Lomeda, C. D. Doyle, D. V. Kosynkin, W. F. Hwang and J. M. Tour, *J. Am. Chem. Soc.*, 2008, **130**, 16201–16206.
3 M. Fathizadeh, W. W. L. Xu, F. Zhou, Y. Yoon and M. Yu, *Adv. Mater. Interfaces*, 2017, **4**, 1600918.
4 F. M. Kafiah, Z. Khan, A. Ibrahim, R. Karnik, M. Atieh and T. Laoui, *Desalination*, 2016, **388**, 29–37.
5 M. Fathizadeh, N. Tien, K. Khivantsev, Z. Song, F. Zhou and M. Yu, *Desalination*, 2017, DOI: 10.1016/j.desal.2017.07.014.
6 M. Hu and B. X. Mi, *Environ. Sci. Technol.*, 2013, **47**, 3715–3723.
7 Y. P. Tang, D. R. Paul and T. S. Chung, *J. Membr. Sci.*, 2014, **458**, 199–208.
8 P. Z. Sun, M. Zhu, K. L. Wang, M. L. Zhong, J. Q. Wei, D. H. Wu, Z. P. Xu and H. W. Zhu, *ACS Nano*, 2013, **7**, 428–437.
9 C. H. Tsou, Q. F. An, S. C. Lo, M. De Guzman, W. S. Hung, C. C. Hu, K. R. Lee and J. Y. Lai, *J. Membr. Sci.*, 2015, **477**, 93–100.
10 H. W. Kim, H. W. Yoon, S. M. Yoon, B. M. Yoo, B. K. Ahn, Y. H. Cho, H. J. Shin, H. Yang, U. Paik, S. Kwon, J. Y. Choi and H. B. Park, *Science*, 2013, **342**, 91–95.
11 R. K. Joshi, P. Carbone, F. C. Wang, V. G. Kravets, Y. Su, I. V. Grigorieva, H. A. Wu, A. K. Geim and R. R. Nair, *Science*, 2014, **343**, 752–754.
12 H. B. Huang, Y. Y. Mao, Y. L. Ying, Y. Liu, L. W. Sun and X. S. Peng, *Chem. Commun.*, 2013, **49**, 5963–5965.
13 A. Akbari, P. Sheath, S. T. Martin, D. B. Shinde, M. Shaibani, P. C. Banerjee, R. Tkacz, D. Bhattacharyya and M. Majumder, *Nat. Commun.*, 2016, **7**, 10891.
14 H. Li, Z. N. Song, X. J. Zhang, Y. Huang, S. G. Li, Y. T. Mao, H. J. Ploehn, Y. Bao and M. Yu, *Science*, 2013, **342**, 95–98.
15 M. Fathizadeh, A. Aroujalian, A. Raisi and M. Fotouhi, *Desalination*, 2013, **314**, 20–27.
16 M. Abedi, M. P. Chenar and M. Sadeghi, *Fibers Polym.*, 2015, **16**, 788–793.
17 G. J. Zhang, H. Meng and S. L. Ji, *Desalination*, 2009, **242**, 313–324.
18 N. Wei, X. S. Peng and Z. P. Xu, *ACS Appl. Mater. Interfaces*, 2014, **6**, 5877–5883.
19 D. Quere, *Annu. Rev. Mater. Res.*, 2008, **38**, 71–99.
20 W. Xu, C. Fang, F. Zhou, Z. Song, Q. Liu, R. Qiao and M. Yu, *Nano Lett.*, 2017, **5**, 2928–2933.
21 D. Cohen-Tanugi, L. C. Lin and J. C. Grossman, *Nano Lett.*, 2016, **16**, 1027–1033.
22 J. J. Song, Y. Huang, S. W. Nam, M. Yu, J. Heo, N. Her, J. R. V. Flora and Y. Yoon, *Sep. Purif. Technol.*, 2015, **144**, 162–167.
23 Q. Nan, P. Li and B. Cao, *Appl. Surf. Sci.*, 2016, **387**, 521–528.
24 L. Qiu, X. H. Zhang, W. R. Yang, Y. F. Wang, G. P. Simon and D. Li, *Chem. Commun.*, 2011, **47**, 5810–5812.

25 W. W. L. Xu, C. Fang, F. L. Zhou, Z. N. Song, Q. L. Liu, R. Qiao and M. Yu, *Nano Lett.*, 2017, **17**, 2928–2933.
26 D. W. Kolpin, E. T. Furlong, M. T. Meyer, E. M. Thurman, S. D. Zaugg, L. B. Barber and H. T. Buxton, *Environ. Sci. Technol.*, 2002, **36**, 1202–1211.
27 S. A. Snyder, P. Westerhoff, Y. Yoon and D. L. Sedlak, *Environ. Eng. Sci.*, 2003, **20**, 449–469.
28 J. Radjenovic, M. Petrovic, F. Ventura and D. Barcelo, *Water Res.*, 2008, **42**, 3601–3610.